national accelerator laboratory

NAL-Pub-74/29-THY
C00-881-404
March 1974

Lepton Pair Production in Hadron-Hadron Collisions

H. P. PAAR*
Columbia University, New York 10027

and

E. A. PASCHOS
National Accelerator Laboratory, Batavia, Illinois 60510
and
University of Wisconsin †, Madison, Wisconsin 53706

ABSTRACT

Lepton production in hadron-hadron collisions is studied in a class of models. In the conventional quark-antiquark anihilation mechanism, the parton distributions incorporate the latest experimental information. The numerical estimates bring out unique signatures and represent realistic upper bounds. In studying the dependence of the results on different quark schemes we find that in models with charm the results remain practically unchanged, or are reduced by a multiplicative factor. We conclude that should the rates be considerably larger than the estimates, then they must be attributed to another origin.

*Research sponsored by the National Science Foundation.

†Supported in part by the University of Wisconsin Research Committee with funds granted by the Alumni Research Foundation, and in part by the U.S. Atomic Energy Commission under Contract AT(11-1)-881, C00-881-404.

Operated by Universities Research Association Inc. Under Contract with the United States Atomic Energy Commission

INTRODUCTION

Ever since the original BNL-Columbia experiment[1] and the Drell and Yan suggestion[2] that the production of heavy lepton pairs can be described within the framework of the parton model there have been numerous efforts trying to observe such processes. The interest is justified on several accounts. From the experimental point[1,3] of view the electromagnetic production of lepton-antilepton pairs is important in normalizing other even more interesting pairs like $e^{+}\nu_{e}$ and $\mu^{+}\nu_{\mu}$. From the theoretical point of view,[2,4-11] the original suggestion gives results similar to those obtained as if the product of the currents is dominated by free field theory singularities,[12] but the justification of the light cone dominance in this process has never been complete. Even within the parton model the numerical estimates depend so critically on the assumptions governing the antiquark distributions, that a conclusive test of the original idea has not been performed and must wait further experimental information. Alternatively, the experiments will determine antiquark distributions which must then be compared with the constraints imposed by other reactions.

In the past year experimental results from neutrino and antineutrino experiments[13,14] indicate that the mean momentum carried by the antiquarks (non-strange) is small. This implies that the production of lepton-pairs is greatly suppressed at large values of Q^2 and it provides a unique signature for the process. The need for an updated calculation is further enhanced by the observation that most of the calculations are concerned with the cross section $\frac{d\sigma}{dQ^2}$, which is not the quantity measured directly in the experiments. What are measured instead are double and triple differential cross sections, subject to experimental efficienty limitations. These reasons compelled us to undertake this investigation of updating the calculation and studying its sensitivity on the underlying assumptions.

In section two we present general formulas which can easily be adapted to diverse experimental situations. Parton distributions which incorporate the latest experimental information are also incorporated in the analysis. Section III gives a wide class of numerical estimates, pointing out signatures unique to this process. We have made an effort to present the expectations of the parton model in detail, so that a direct test with experiment is possible. If the experimental measurements are in the vicinity of the estimates then the pursue of further tests and correlations is desirable. If, on the other hand, the measurements are considerably larger than the estimates, then we must seek an alternative explanation.[15] The parton contribution may still be there and a two arm spectrometer could search for it. Section IV discusses briefly the effects of nuclear corrections, integrally charged quarks, charmed quarks and the direct production of charmed particles.

GENERAL FORMULAS

Consider the reactions

$$p(p_+) + p(p_-) \rightarrow \ell\,(q_+) + \bar{\ell}(q_-) + \Gamma \qquad (2.1)$$

where $\ell - \bar{\ell}$ is a lepton-antilepton pair, like e^+e^-, $\mu^+\mu^-$, and Γ is any combination of hadronic states. The original Drell-Yan model[2] visualizes the scattering to proceed through quark-antiquark anihilation into leptons. The kinematics are defined as follows

$$S = (p_+ + p_-)^2 \qquad (2.2)$$

$$Q^2 = (q_+ + q_-)^2 \approx xx'S \qquad (2.3)$$

while some of the other variables are defined in Fig. 1. The variables x and x' are given in terms of invariants

$$x = \frac{2}{S}[p_- \cdot q_+ + p_- \cdot q_-] \qquad (2.4)$$

$$x' = \frac{2}{S}[p_+ \cdot q_+ + p_+ \cdot q_-] \qquad (2.5)$$

Cross sections for such processes have been derived following standard techniques. It is useful to write a cross section, which is invariant under Lorentz transformations along the beam direction

$$q_+^\circ \frac{d\sigma}{d q_+^3} = \frac{8\alpha^2}{S^2 Q^4} \left\{ (p_+ \cdot q_+)(p_- \cdot q_-) + (p_+ \cdot q_-)(p_- \cdot q_+) \right\} \frac{d\cos\theta_-}{\sin^2\theta_-} \Phi(x, x') \qquad (2.6)$$

where α is the fine structure constant $\Phi(x, x')$ is a function of the parton distributions to be defined explicitly in the latter part of this section. The volume element $\frac{d\cos\theta_-}{\sin^2\theta_-}$ is invariant under boosts along the beam direction. Triple differential cross sections are obtained readily either in the laboratory frame

$$\frac{d^3\sigma}{d\,q^\circ\, d\cos\theta_+ d\cos\theta_-} = \frac{8\pi\alpha^2}{SQ^4}\, q_+^3 \frac{\sin\theta_+}{\sin^3\theta_-}\left\{2 - \cos\theta_+ + \cos\theta_-\right\}\,\Phi(x,x') \tag{2.7}$$

or the center of mass frame

$$\frac{d^3\sigma}{d\,q^\circ\, d\cos\theta_+ d\cos\theta_-} = \frac{8\pi\alpha^2}{SQ^4}\, q_+^3 \frac{\sin\theta_+}{\sin^3\theta_-}\left\{1 + \cos\theta_+ \cdot \cos\theta_-\right\}\,\Phi(x,x') \tag{2.8}$$

The basic assumption of parton-antiparton anihilation has several consequences. In the limit where the transverse momenta of the constituents are neglected (i) the plane formed by the dilepton pair contains the beam direction, and (ii) the transverse momentum of the dilepton pair is zero, i.e.,

$$q_-\sin\theta_- = q_+\sin\theta_+ \quad . \tag{2.9}$$

Violations of this relation, arising from a perpendicular momentum dependence in the parton distribution, should be limited to a few hundred MeV. Most of the interesting physics is hidden in the function $\Phi(x,x')$, which is discussed next.

The overlap function $\Phi(x,x')$ is defined by

$$\Phi(x,x') = \sum_\ell f_\ell(x)\, f_{\bar\ell}(x')\, Q_\ell^2 + \sum_\ell f_\ell(x')\, f_{\bar\ell}(x)\, Q_{\bar\ell}^2 \tag{2.10}$$

while the electroproduction structure function is

$$F_2(x) = x \sum_{\ell} Q_{\ell}^2 f_{\ell}(x) + x \sum_{\bar{\ell}} Q_{\bar{\ell}}^2 f_{\bar{\ell}}(x) \qquad (2.11)$$

where $\sum_{\ell}$ and $\sum_{\bar{\ell}}$ imply summations over quarks and antiquarks, respectively. There are, however, several measurements which indicate that the momentum carried by the antipartons and the strange quarks is much smaller that the momentum carried by the non-strange partons. The observed ratio of the antineutrino to neutrino total cross sections on matter satisfies

$$\frac{\sigma^{\bar{\nu}}}{\sigma^{\nu}} = \frac{1}{3}(1+\epsilon) \qquad (2.12)$$

where $$\epsilon = \begin{cases} 0.132 & \text{for } 1 \le E \le 10 \text{ GeV} \\ 0.120 & \text{for } \quad E \le 80 \text{ GeV} \end{cases}$$

for $\sin^2\theta_c = 0$ this implies[16]

$$\sum_{\bar{\ell}}{}' \int x\, f_{\bar{\ell}}(x)\, dx \le \frac{3}{8}\, \epsilon \sum \int x\, f_{\ell}(x) dx + O(\epsilon^2) \qquad (2.13)$$

where the Σ' indicates summations over quarks or antiquarks which couple to the $\Delta S = 0$ part of the weak current. If in addition $\sigma_S/\sigma_T = 0$ in neutrino induced reactions, then (2.13) becomes an equality. We do not make this additional assumption, because the corresponding ratio determined in electroproduction is different from zero. The main result is that the contribution of the non-strange quarks is limited to small x. It is supposed that x is small enough so that the diffraction formula[7] holds

$$f_{\bar{p}}(x) = f_{\bar{n}}(x) \simeq \frac{a}{x} G(x) \qquad (2.14)$$

where G(x) is a function with G(o) = 1 and decreasing rapidly with x .

To determine the significance of the strange quarks one must compare the electropoduction to neutrino results. The ratios[16,17]

$$\frac{\int \left[F_2^{\gamma n} + F_2^{\gamma p}\right] dx}{\int \left[F_2^{\nu n} + F_2^{\nu p}\right] dx} = 0.30 \pm 0.06 \leq \frac{5}{18} + \sigma \qquad (2.15)$$

and

$$\frac{\int \left[F_2^{\gamma n} + F_2^{\gamma p}\right] x dx}{\int \left[F_2^{\nu n} \quad F_2^{\nu p}\right] x dx} \lesssim 0.32 \qquad (2.16)$$

bound the strange quark contribution

$$\frac{\int x \left[f_\lambda + f_{\bar{\lambda}}\right] dx}{\int x \left[f_p + f_{\bar{p}} + f_n + f_{\bar{n}}\right] dx} \lesssim 9\sigma = 0.7 \qquad (2.17)$$

$$\frac{\int x^2 \left\{f_\lambda + f_{\bar{\lambda}}\right] dx}{\int x^2 \left[f_p + f_{\bar{p}} + f_n + f_{\bar{n}}\right] dx} \lesssim 0.4 \qquad (2.18)$$

The bounds indicate that the strange quark contribution is also peaked at small values of x . They suggest that f_λ and $f_{\bar{\lambda}}$ may be limited in the diffractive region, but they are not stringent enough to imply this conclusion. We shall also assume that

$$f_{\bar{\lambda}}(x) = \frac{b}{x} G'(x)$$

where b is a constant and $G'(x)$ is again a rapidly decreasing function of x with $G'(o) = 1$. Point by point comparisons between $F_2^{\gamma}(x)$ and $F_2^{\nu}(x)$ will determine the importance of the strange and non-strange structure functions. In the absence of such detailed information we shall take $a = b$ and $G(x) = G'(x)$ leading to

$$f_{\bar{p}}(x) = f_{\bar{n}}(x) = f_{\bar{\lambda}}(x) = \frac{a\,G(x)}{x} \quad . \tag{2.19}$$

We believe that the ambiguities arising from the specific form of $G(x)$ are far greater than those arising from equating all the antiquark structure functions. In any case, evidence of the limited antiquark distributions should be present in the numerical estimates. From (2.10); (2.11) and 2.19) we obtain

$$xx' \Phi(x, x') = \frac{F_2(o)}{2\sum_{\ell} Q_{\ell}^2} \left\{ F_2(x)\, G(x') + F_2(x')\, G(x) - F_2(o) G(x) G(x') \right\} \tag{2.20}$$

where $a = \frac{F_2(o)}{2\sum_{\ell} Q_{\ell}^2}$ has also been used. Quark models where the antiquark distributions satisfy (2.19) will lead to a formula of this form. The functional form is similar to the one suggested by Gronau.[18] The main difference stems from the fact that we do not have to restrict the experiments to kinematic regions where x and x' are small, since nature automatically provides such a restriction for the antiquark distributions.

There are two other formulas which occur frequently in articles. The double diffectial cross section[19] in the center-of-mass system

$$\frac{d\sigma}{dQ^2 dQ_{\parallel}} = \frac{8\pi\alpha^2}{3Q^4} \frac{Q_{\parallel} + \sqrt{Q_{\parallel}^2 + Q^2}}{\left(Q_{\parallel} + \sqrt{Q_{\parallel}^2 + Q^2}\right)^2 + Q^2} \quad xx'\Phi(x, x') \tag{2.21}$$

and the Drell-Yan formula[2]

$$\frac{d\sigma}{dQ^2} = \frac{4}{3} \frac{\pi\alpha^2}{Q^2 S} \int \Phi\left(x, \frac{Q^2}{sx}\right) \frac{dx}{x} \tag{2.22}$$

We shall use these formulas in the next section in order to obtain estimates for a variety of experimental situations.

NUMERICAL ESTIMATES

In estimating the cross sections a choice must be made for the quantities $\sum_\ell Q_\ell^2$ and $G(x)$. Asymptotically the sum of the squares of the quark charges is related to the electron-positron anihilation[20] as follows

$$\sum_\ell Q_\ell^2 = \frac{\sigma(e^+e^- \rightarrow \text{hadrons})}{\sigma(e^+e^- \rightarrow \mu^+\mu^-)} \tag{3.1}$$

Present data do not seem to indicate a constant ratio associated with asymptopia. However, in production experiments the dilepton masses are so much larger that an asymptotic region could still make sense. Quark models give a wide range of values. For the estimates we shall select the value of $\sum_\ell Q_\ell^2 = 2/3$, corresponding to Gell-Mann-Zweig quarks.

To accentuate the cut off in momentum distributions we chose

$$G(x) = \theta(\xi - x) \tag{3.2}$$

with $\xi = 0.10$ and 0.20 . We have also chosen a $G(x)$ obtained in explicit parametrizations of electroproduction and neutrino induced data. Parametrizations[21] satisfying the sum rules and threshold behavior give

$$G(x) = (1-x)^\eta \tag{3.3}$$

with $\eta \simeq 9$. In order to study the sensitivity of the results on the functional forms of $G(x)$ we varied ξ and the exponent η. Additional quantum numbers like color or charm will further reduce the cross sections. The effect of m such multiplets is to scale down the results by an overall factor $1/m$.

In the BNL-Columbia experiment[1] μ-pairs were observed with a longitudinal momentum $\gtrsim 12$ (GeV/c). Theoretical curves,* which account for this experimental constraint, are shown in Fig. 2. For $\xi = 0.20$ and $Q \lesssim 2.5$ GeV the theoretical curve could be compatible with experimental points. Significant deviations occur for larger values of Q.

Figure 3 shows the invariant and scaling quantity $Q^2 s \frac{d\sigma}{dQ^2}$ as function of $\tau = Q^2/s$ for different parameterizations of $G(x)$. We note that for small τ the shapes and normalizations of the curves are very similar. Substantial differences arise at larger values of τ. In the same figure is shown an upper bound from the CCR experiment.[3] All the estimates are consistent with the bound.

Estimates for the double differential cross section [e.g., (2.21) in the center of mass system are shown in Fig. 4. An important signature, arising from the limitation of the antiquark momentum, is the substantial leveling (dashed curve) and perhaps decrease (solid curve) of the cross section at small $Q_{||}$.

---

*We were informed that M. Einhorn and R. Savit are completing work related to this cross section. (NAL-Pub-74/35-THY).

In experiments of the NAL-type one arm spectrometers seem to be favored. For such configurations we integrate over θ_- and present the results as functions of θ_+ and q_+. Figures 5-7 show such curves* for different parametric forms of G(x). We note that for small momentum of the observed lepton, the dependence on G(x) is not critical, but it becomes more important as the momentum increases.[22] Figure 8 shows the dependence of the double differential cross section on the parameter η occuring in (3.3). In a two arm spectrometer one would like to set q_+ and θ_+ at specific values and search for the other lepton at places where the cross section has a maximum. Several such curves are shown in Fig. 9. The main feature in this case is a narrow angular band of θ_-, into which most of the events are concentrated.

---

*We have ascertained that throughout the range of integration Q^2 remains large enough for the model to be valid.

CONCLUSIONS AND REMARKS

So far we presented a detailed discussion of the Drell-Yan model in view of the prevailing quark-parton ideas. We have gone into some detail in presenting numerical estimates so that a direct comparison would be possible. The numerical results should still be considered as estimates, because the antiquark contributions could be considerably smaller and diminish the total rate even further. The antiquark contributions cannot be larger than the cases we discussed. Thus an abnormally high rate will have to come from an alternative explanation. Several other effects could also be present and we shall elaborate on some of them.

Nuclear Corrections: The experiments are done in nuclei and nuclear corrections could be important. The most important one seems to be the production of pions on the surface of the nucleus, which subsequently produce leptons through the reaction

$$\pi + \text{matter} \rightarrow \ell\bar{\ell} + \text{anything} \quad . \tag{4.1}$$

This effect could be analysed as a two step process. First the mesons are produced which then rescatter to produce the leptons. Since the antiquark distribution in mesons is not expected to be limited to small x the $p_\perp$ dependence of the leptons is expected to be considerably different.[23]

Integrally Charged Quarks: Considering again the basic interaction to be

$$q + \bar{q} \rightarrow \ell + \bar{\ell} \qquad (4.1)$$

we can inquire whether different representations of quarks could lead to considerably different conclusions. A representative case is three integrally charged triplets of the Han-Nambu[24] type. Limitations on the non-strange antiquark distributions again follow from a helicity argument and remain unchanged. Detail features in such models depend on the specific structure of the weak and electromagnetic currents. Assuming again that the λ - type quark distributions are limited, we arrive at similar cross sections, except for an overall normalization factor. The cross section is reduced by a factor of 1/3 due to the three multiplets and in addition by the fact that $\Sigma Q_i^2 = 4$ in this case.

Charmed Quarks: Charmed quarks are frequently introduced through the GIM scheme[25]

$$\begin{pmatrix} p \\ n_c \end{pmatrix}_L \quad \text{and} \quad \begin{pmatrix} p' \\ \lambda_c \end{pmatrix}_L \qquad (4.2)$$

where $n_c = n \cos\theta_c + \lambda \sin\theta_c$ and $\lambda_c = -n \sin\theta_c + \lambda \cos\theta_c$. The charged weak currents

$$J^W = \bar{p}n_c + \bar{p}'\lambda_c \tag{4.3}$$

contain transitions into the charmed states. Most likely, low energy neutrino experiments have not excited charmed states. Consequently, the effective form of the structure functions is the same as in the absence of charm. Couplings of the electromagnetic current, on the other hand, do not excite charmed states, so that available determinations of νW_2 must include contributions from charmed quarks.[26] Comparisons among the structure functions in the two processes determines the importance of charmed states. Omitting again the antiquark contributions we arrive at

$$\frac{4f_{p'} + f_\lambda}{f_p + f_n} \leq 9\sigma \tag{4.4}$$

It is now evident that the presence of charmed quarks will not seriously modify the previous results, because the combined λ and p' distributions are limited.

So far we considered conventional quark-models where the quarks are left handed. We could in general consider cases where besides the multiplets (4.2) there are also right-handed multiplets. In such cases the ratio of the cross sections being 1/3 must follow from a detailed choice of the structure functions. The predictions for the production of heavy leptons in this class of models can be quite different.

Other Mechanisms: If charm states exist they should be produced directly in hadronic reactions[27] either singly or in pairs. They can be detected by their leptonic decays. Lepton-antilepton pairs could be produced in this manner, but the correlations and distinct signatures associated with the electromagnetic production of pairs should now be absent.

Other mechanisms like two photon contributions,[28] direct W- production[29,30] and the effects of neutral currents[29-31] have also been studied and we refer to the available articles.

REFERENCES

[1] J. Christenson, et al., Phys. Rev. Letters 25, 1523 (1970).

[2] S. D. Drell and T. M. Yan, Phys. Rev. Letters 25, 316 (1970), and Ann. of Phys. 66, 578 (1971).

[3] B. G. Pope, Report at the 11th Aix-en-Provence Conference (1973).

[4] J. Kuti and V. Weisskopf, Phys. Rev. D4, 3418 (1971).

[5] P. V. Landshoff and J. C. Polkinghorne, Nucl. Phys. B33, 221 (71), and B36, 642 (72).

[6] S. M. Berman, J. D. Bjorken and J. B. Kogut, Phys. Rev. D4, 3388 (1971). For a summary, see: J. D. Bjorken, in Proceedings of the 11th Aix-en-Provence Conf. (1973).

[7] R. P. Feynman, Photon-Hadron Interactions, Benjamin (W. A.), Inc., Reading, Massachusetts (1972).

[8] R. W. Fiddler, Phys. Letters 46B, 455 (1973).

[9] K. J. Evans, Nucl. Phys. B65, 540 (1973).

[10] H. B. Thacker, ITP-73-48, Stony Brook preprint (1973).

[11] G. R. Farrar, Cal. Tech. preprint 68-422 (1974)

[12] K. Wilson compares the two approaches in Proceedings of 1971 Int. Symp. on Electron and Photon Interactions at High Energies, Cornell University (1971). G. Altarelli, R. A. Brandt and G. Preparata, Phys. Rev. Lett. 26, 42 (1971).

[13] T. Eichten, et al., Phys. Lett. 46B, 274 (1973).

[14] A. Benvenutti, et al., Phys. Rev. Lett. 30, 1084 (1973) and 32, 125 (1974).

[15] A larger rate than expected was observed in the reactions

(a) $\gamma p \rightarrow \mu^+\mu^- + x$: J.F. Davis, et al., Phys. Rev. Letters 29, 1356 (1972);

(b) $\gamma p \rightarrow \gamma + x$: D.O. Caldwell et al., preprint 73-3649, Univ. of Cal. at Santa Barbara;

(c) $\mu + p \rightarrow \mu + \gamma + x$: K.C. Königsmann, Univ. of Rochester preprint 471 (1974);

(d) $e^+ + e^- \rightarrow$ hadrons : A. Litke, et al., Phys. Rev. Lett. 30, 1189 (1973); G. Tarnopolsky, Phys. Rev. Lett. 32, 432 (1974), and B. Richter, Invited Talk APS Meeting Chicago, (1974).

[16] E.A. Paschos and V.I. Zakharov, Phys. Rev. D8, 215 (1973); E.A. Paschos, NAL-Conf-73/27-THY (1973).

[17] H.J. Lipkin and E.A. Paschos, Phys. Rev. D8, 2325 (1973).

[18] M. Gronau, Phys. Lett. 39B, 395 (1972).

[19] R. Jaffe and J. Primack (private communication to S.C.C. Ting); C.H. Llewellyn Smith, TH.1710-CERN.

[20] J. D. Bjorken, SLAC-Pub-1318 (1973).

[21] V. Barger and R.J.N. Phillips, University of Wisconsin preprint (1973), (to be published); R. McElhaney and S.F. Tuan, Phys. Rev. D8, 2269 (1973). The antiquark distributions considered are also consistent with

the quark counting arguments of S. J. Brodsky and G. R. Farrar, Phys. Rev. Lett. 31, 1153 (1973).

[22]The results in Fig. 5-8 are relevant to the NAL experiments. A comparison with the BBK-paper (Ref. 6) shows that the two calculations agree for small q_+ ($\leq$ 40 GeV), but they diverge for larger values of q_+. This is expected because $\phi(x, x')$ for the two calculations coincide when both x and x' are small and differ when one of them is large.

[23]Charge exchange nuclear corrections have been found to be important at low energies in several reactions: M. M. Sternheim and R. R. Silbar, Phys. Rev. D6, 8117 (1972); S. L. Adler, S. Nussinov and E. A. Paschos, NAL-Pub-73/86-THY (to be published in Phys. Rev.).

[24]M. Y. Han and Y. Nambu, Phys. Rev. 139, B1006 (1965) and Enrico Fermi Institute preprint 27 (1973).

[25]S. Glashow, J. Iliopoulos, L. Maiani, Phys. Rev. D2, 1285 (1972).

[26]A. De Rújula, H. Georgi, S.L. Glashow and H. R. Quinn, Harvard preprint (1974).

[27]G. Snow, Nucl. Phys. B55, 445 (1973).

[28]M.S. Chen, I. Z. Muzinich, H. Terazawa and T. P. Cheng, Phys. Rev. D7, 3485 (1973).

[29]R.L. Jaffe and J. R. Primack, Nucl. Phys. B61, 317 (1973).

[30]L. M. Lederman and D.H. Saxon, Nucl. Phys. B63, 315 (1973).

[31]R. W. Brown, K.O. Mikaelian and M. K. Gaillard, NAL-Pub-74/14-THY (1974).

FIGURE CAPTIONS

Fig. 1 Kinematics for the process.

Fig. 2 Comparison of the BNL-Columbia experiment with parton model expectations. Solid curve corresponds to $\theta(0.20-x)$ and dashed curve to $(1-x)^9$.

Fig. 3 Comparison with the CCR bound indicated by the arrows. Curves correspond to the parametrizations of G(x) shown in the Figure.

Fig. 4 Double differential cross section in the center of mass system.

Fig. 5 Double differential cross section in the laboratory frame for different incident energies and angles θ_+. For all the curves $G(x) = \theta(0.10-x)$.

Fig. 6 Same as in Fig. 5, but for $G(x) = \theta(0.20-x)$.

Fig. 7 Same as in Fig. 5, but for $G(x) = (1-x)^9$.

Fig. 8 Double differential cross section in the laboratory frame at the angles $\theta_+ = 40$ and 80 miliradians. Three different parametrizations of G(x) are shown.

Fig. 9 Triple differential cross section in the laboratory frame for $G(x) = (1-x)^9$.

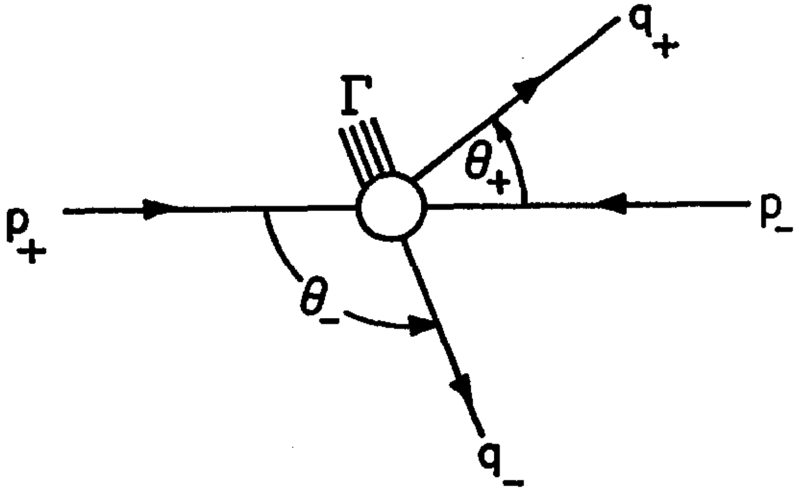

Fig. 1

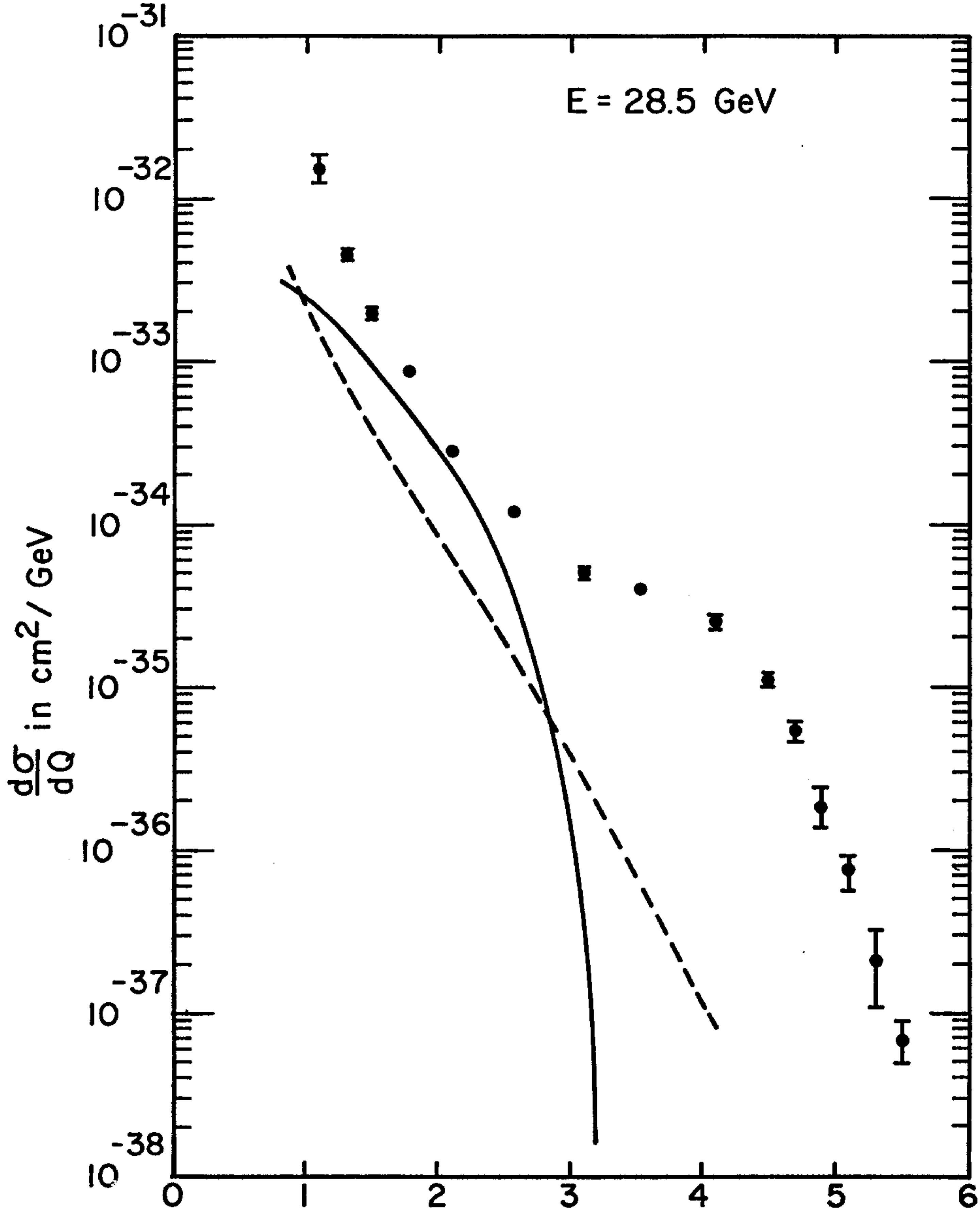
E = 28.5 GeV
$\frac{d\sigma}{dQ}$ in cm^2/ GeV
Q GeV
10^{-31}
10^{-32}
10^{-33}
10^{-34}
10^{-35}
10^{-36}
10^{-37}
10^{-38}
0
1
2
3
4
5
6

Fig. 2

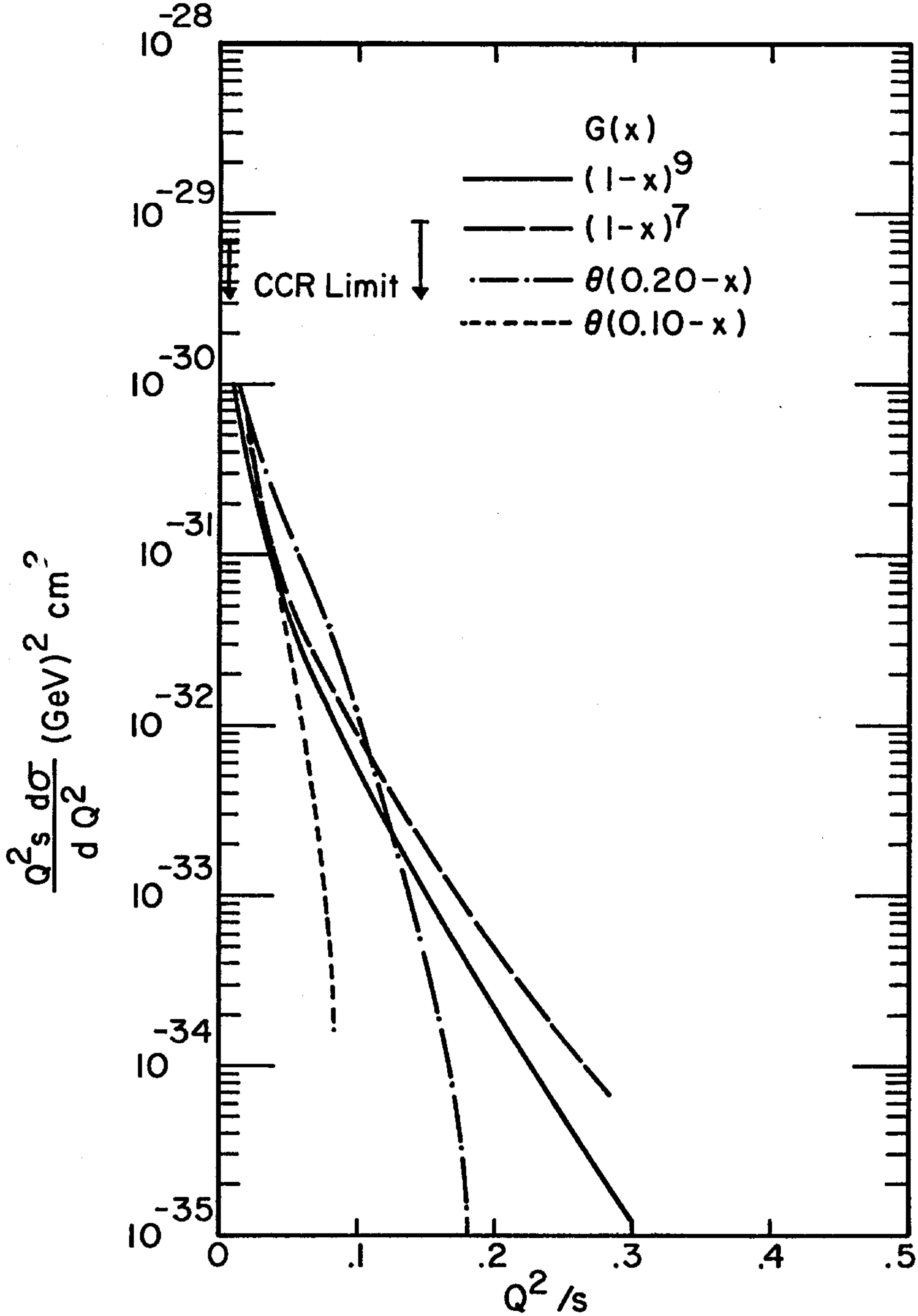

G(x)
$(1-x)^9$
$(1-x)^7$
$\theta(0.20-x)$
$\theta(0.10-x)$
CCR Limit
10^{-28}
10^{-29}
10^{-30}
10^{-31}
10^{-32}
10^{-33}
10^{-34}
10^{-35}
0
.1
.2
.3
.4
.5
Q^2/s
$\frac{Q^2 s\, d\sigma}{d Q^2}$ $(\mathrm{GeV})^2\ \mathrm{cm}^2$

Fig. 3

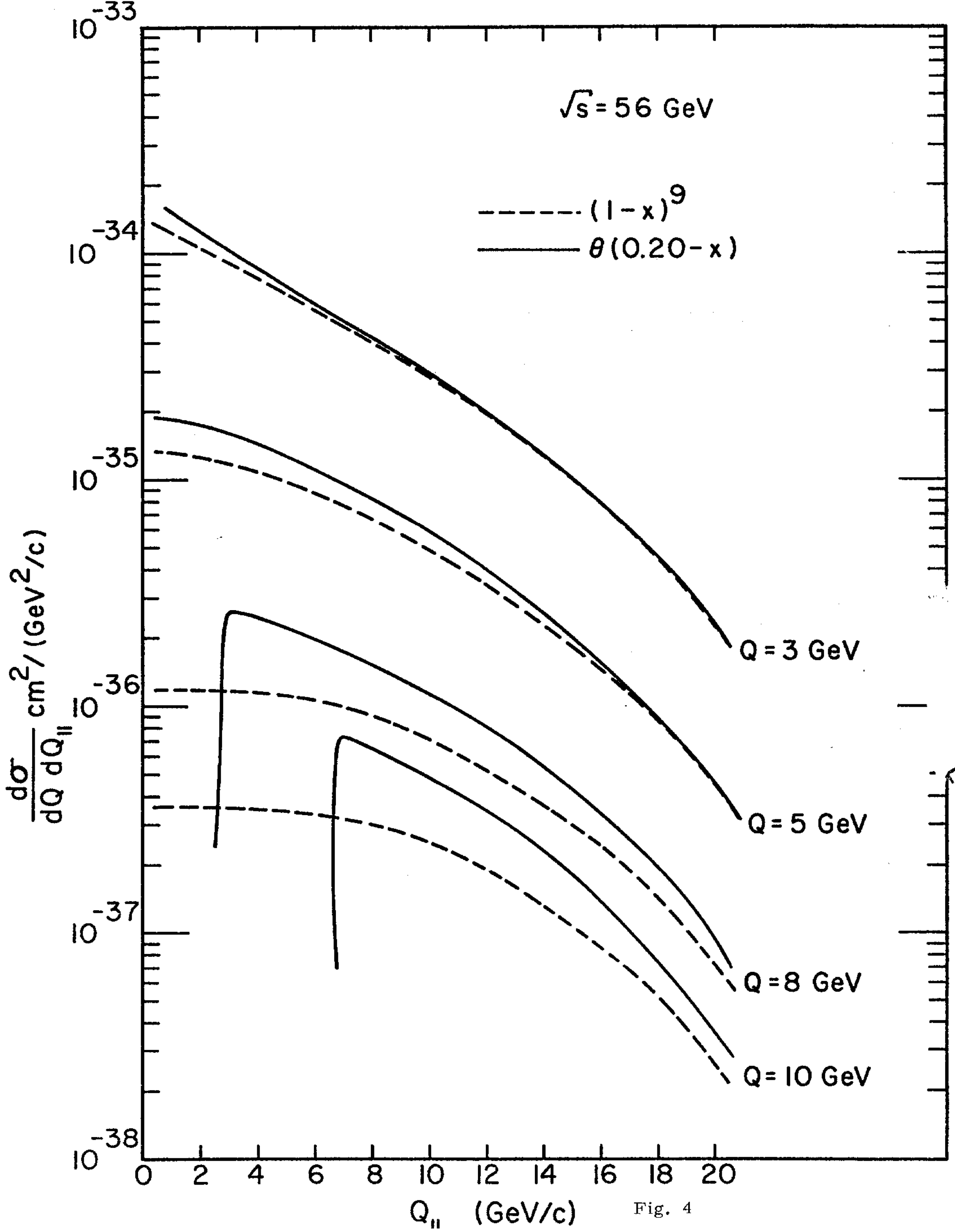
$\sqrt{s} = 56$ GeV
$(1-x)^9$
$\theta(0.20-x)$
Q = 3 GeV
Q = 5 GeV
Q = 8 GeV
Q = 10 GeV
10^{-33}
10^{-34}
10^{-35}
10^{-36}
10^{-37}
10^{-38}
0 2 4 6 8 10 12 14 16 18 20
$Q_{\parallel}$ (GeV/c)
$\frac{d\sigma}{dQ\,dQ_{\parallel}}$ cm^2/(GeV^2/c)

Fig. 4

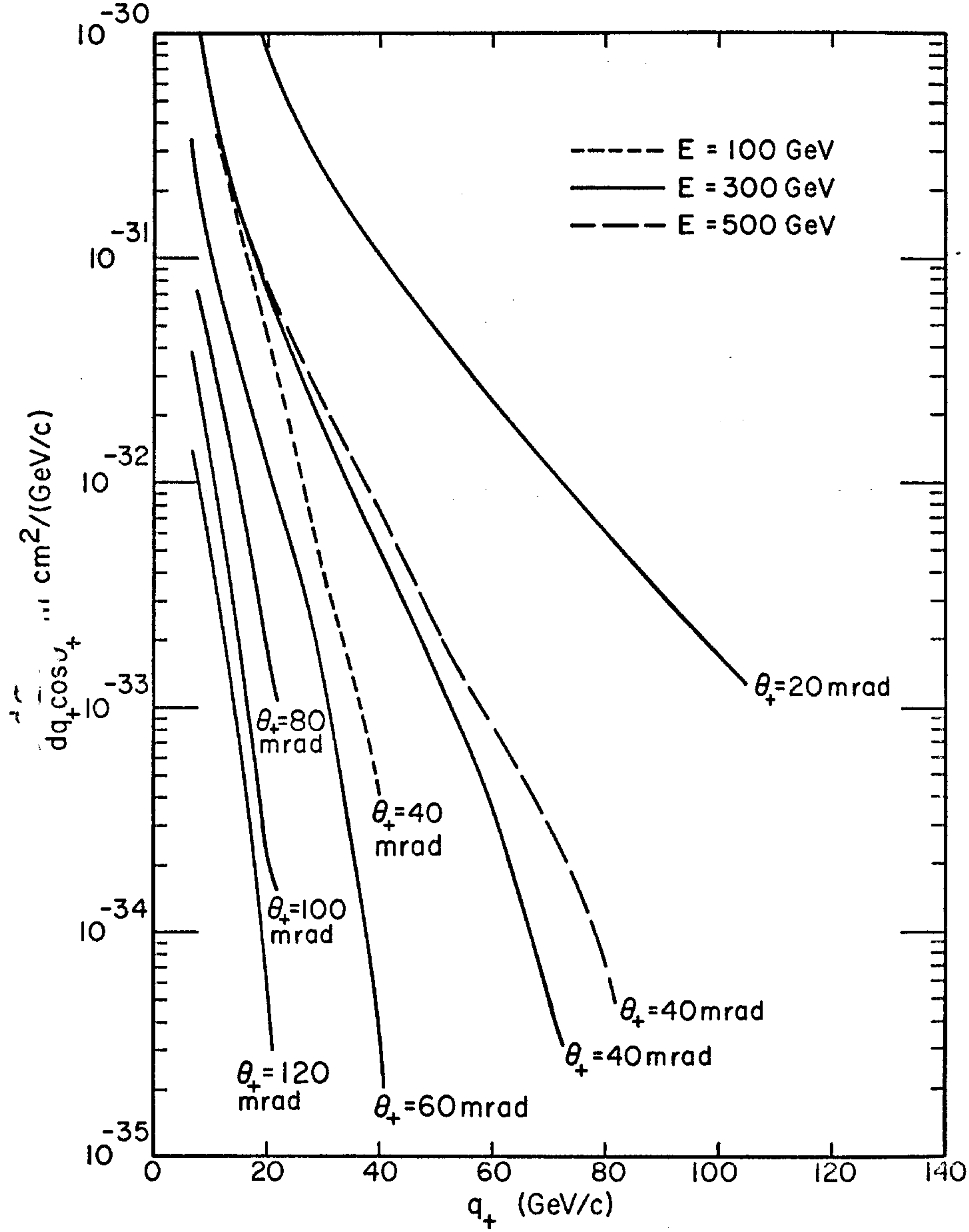
E = 100 GeV
E = 300 GeV
E = 500 GeV
θ_+=20 mrad
θ_+=80 mrad
θ_+=40 mrad
θ_+=100 mrad
θ_+=40 mrad
θ_+=40 mrad
θ_+=120 mrad
θ_+=60 mrad
10^{-30}
10^{-31}
10^{-32}
10^{-33}
10^{-34}
10^{-35}
0
20
40
60
80
100
120
140
q_+ (GeV/c)
cm^2/(GeV/c)

Fig. 5

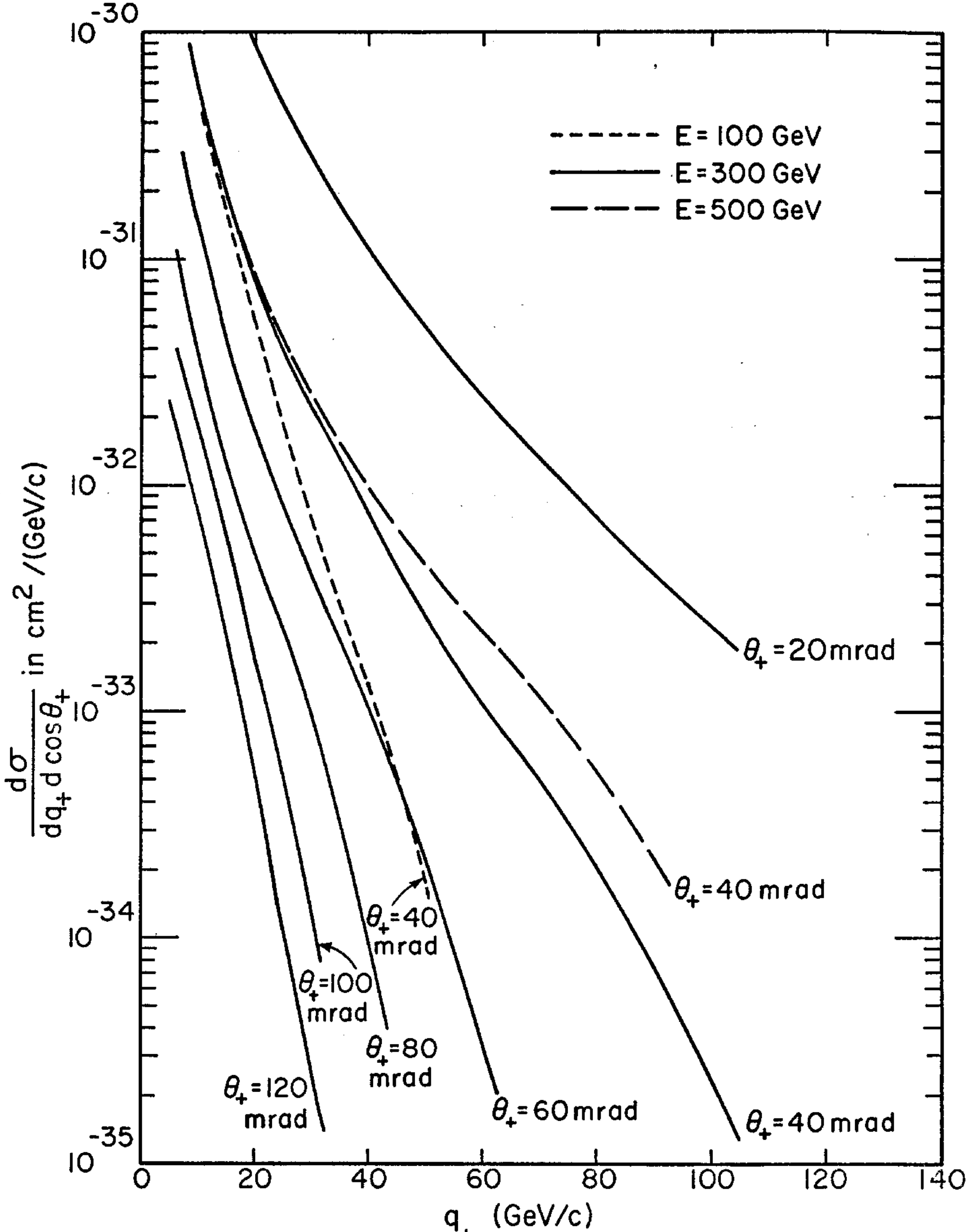

E = 100 GeV
E = 300 GeV
E = 500 GeV
$\theta_+ = 20$ mrad
$\theta_+ = 40$ mrad
$\theta_+ = 40$ mrad
$\theta_+ = 60$ mrad
$\theta_+ = 80$ mrad
$\theta_+ = 100$ mrad
$\theta_+ = 120$ mrad
$\theta_+ = 40$ mrad
10^{-30}
10^{-31}
10^{-32}
10^{-33}
10^{-34}
10^{-35}
0
20
40
60
80
100
120
140
q_+ (GeV/c)
$\frac{d\sigma}{dq_+ \, d\cos\theta_+}$ in cm^2 /(GeV/c)

Fig. 6

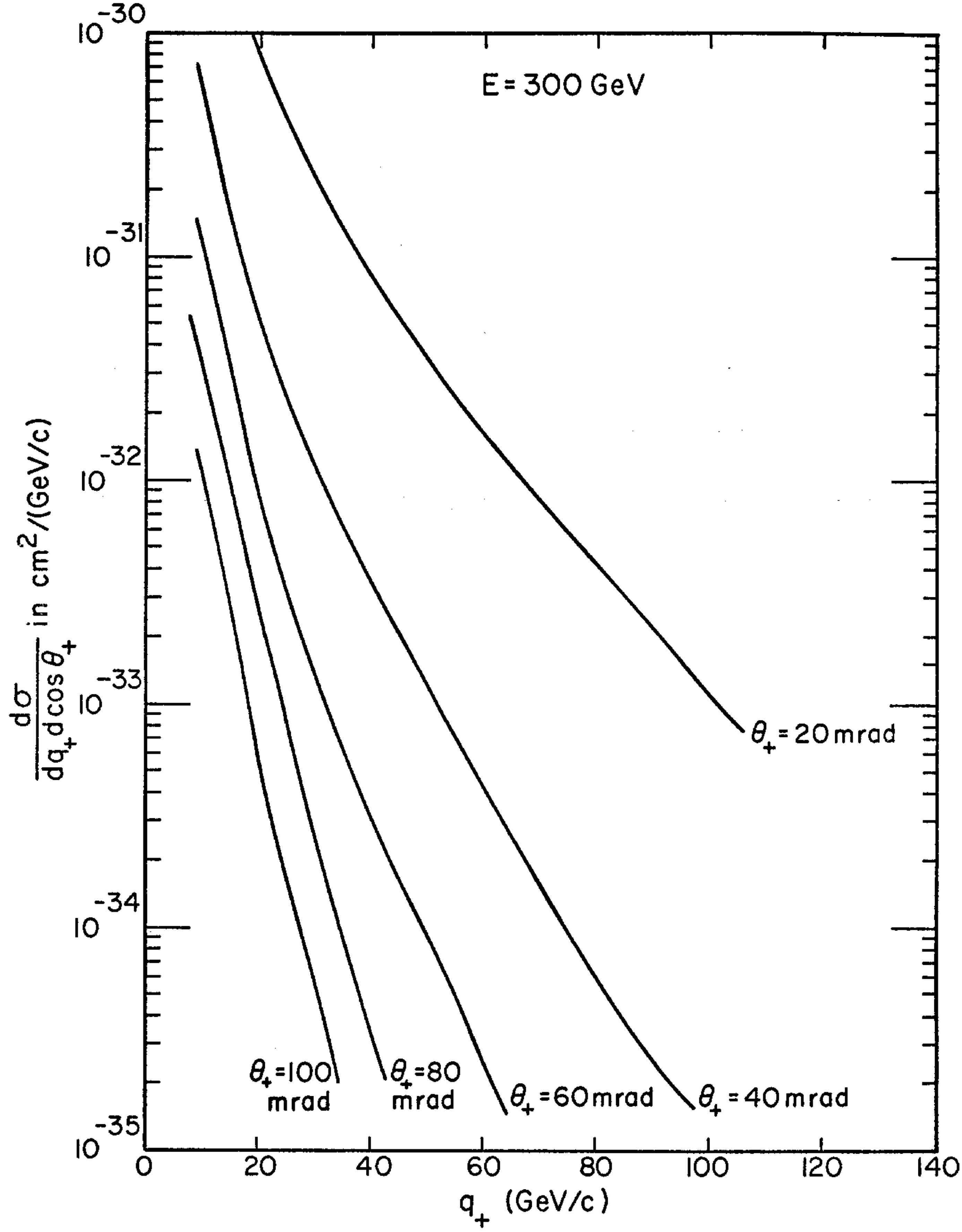
E = 300 GeV
$\frac{d\sigma}{dq_+ d\cos\theta_+}$ in cm^2/(GeV/c)
10^{-30}
10^{-31}
10^{-32}
10^{-33}
10^{-34}
10^{-35}
$\theta_+ = 20$ mrad
$\theta_+ = 100$ mrad
$\theta_+ = 80$ mrad
$\theta_+ = 60$ mrad
$\theta_+ = 40$ mrad
0
20
40
60
80
100
120
140
q_+ (GeV/c)

Fig. 7

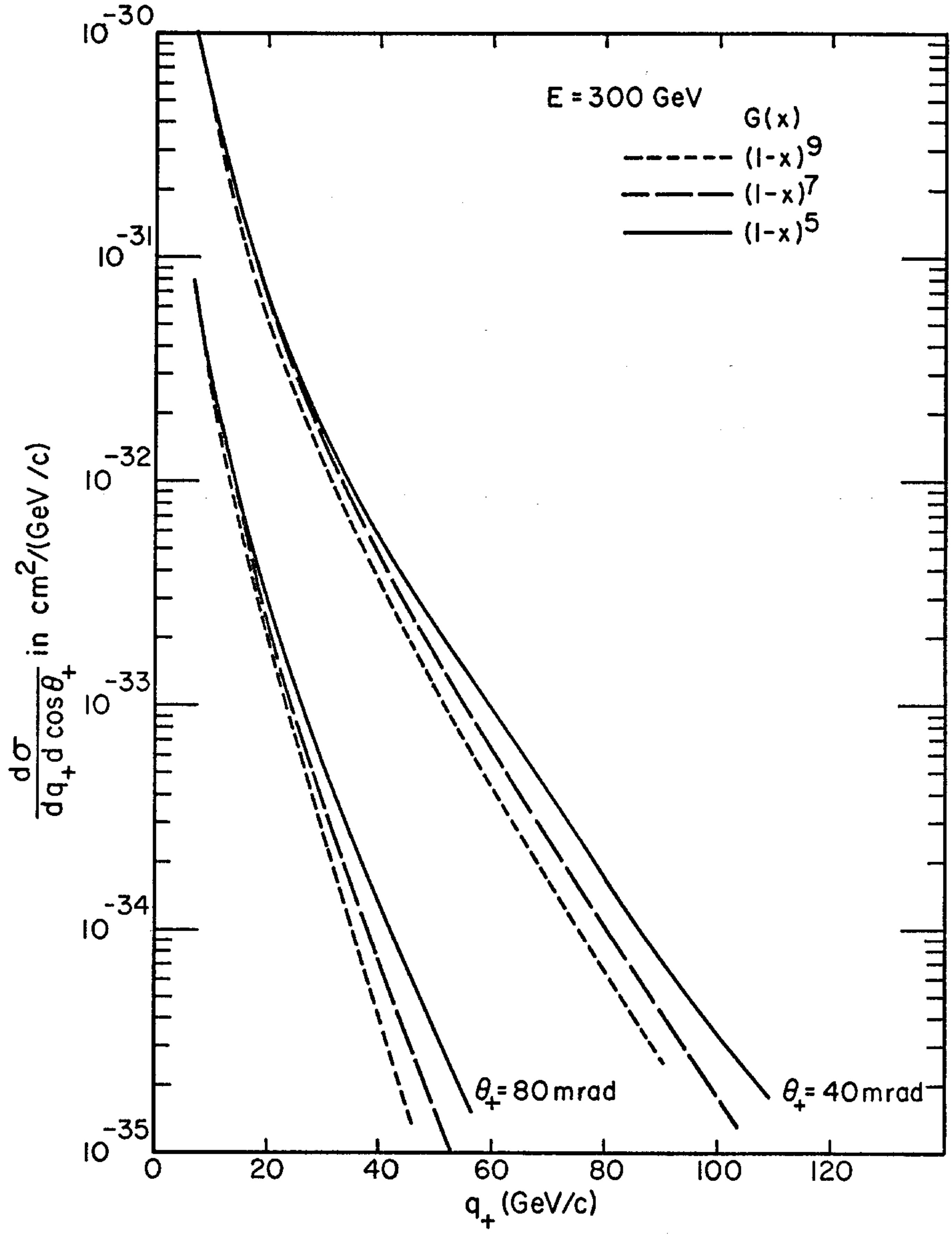

E = 300 GeV
G(x)
(1-x)^9
(1-x)^7
(1-x)^5
θ+ = 80 mrad
θ+ = 40 mrad
10^-30
10^-31
10^-32
10^-33
10^-34
10^-35
0
20
40
60
80
100
120
q+ (GeV/c)
dσ/(dq+ d cos θ+) in cm^2/(GeV/c)

Fig. 8

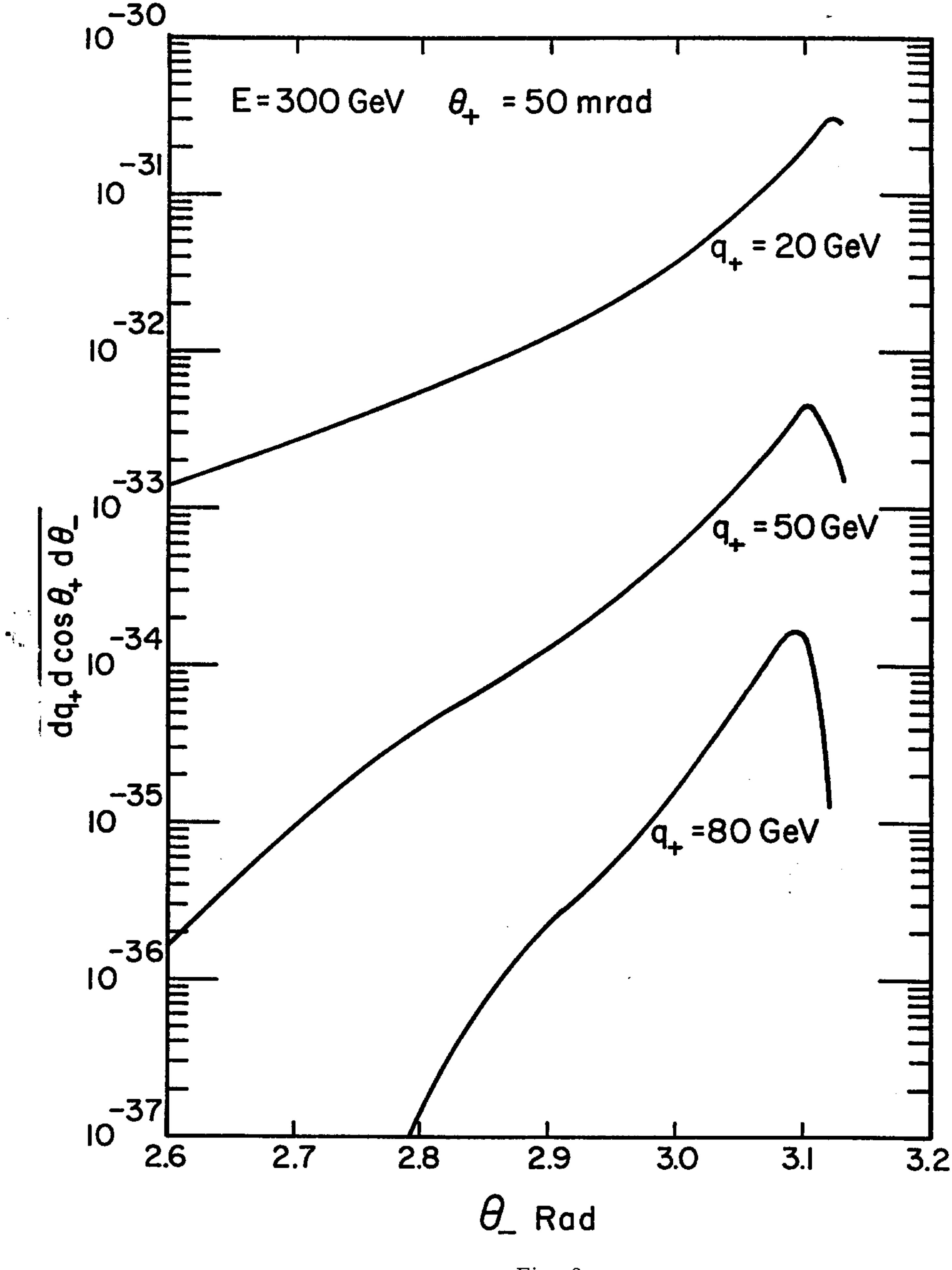
E = 300 GeV θ_+ = 50 mrad
q_+ = 20 GeV
q_+ = 50 GeV
q_+ = 80 GeV
$\frac{d\sigma}{dq_+ \, d\cos\theta_+ \, d\theta_-}$
10^{-30}
10^{-31}
10^{-32}
10^{-33}
10^{-34}
10^{-35}
10^{-36}
10^{-37}
2.6
2.7
2.8
2.9
3.0
3.1
3.2
θ_- Rad

Fig. 9